Journal of Marine Science and Technology

Volume 24 | Issue 2 Article 10

CORROSION OF REBAR UNDER CARBONATION AND SALT ENVIRONMENT

Wei-Chung Yeih
Department of Harbor and River Engineering, National Taiwan Ocean University, Keelung, Taiwan, R.O.C

Jiang-Jhy Chang
Department of Harbor and River Engineering, National Taiwan Ocean University, Keelung, Taiwan, R.O.C., jjc@mail.ntou.edu.tw

Yu-Ping Huang
Department of Harbor and River Engineering, National Taiwan Ocean University, Keelung, Taiwan, R.O.C.

Ran Huang
Department of Harbor and River Engineering, National Taiwan Ocean University, Keelung, Taiwan, R.O.C.

Recommended Citation

Yeih, Wei-Chung; Chang, Jiang-Jhy; Huang, Yu-Ping; and Huang, Ran (2016) "CORROSION OF REBAR UNDER CARBONATION AND SALT ENVIRONMENT," *Journal of Marine Science and Technology*: Vol. 24: Iss. 2, Article 10.
DOI: 10.6119/JMST-015-0629-2
Available at: https://jmstt.ntou.edu.tw/journal/vol24/iss2/10

CORROSION OF REBAR UNDER CARBONATION AND SALT ENVIRONMENT

Acknowledgements

This work was supported by National Science Council, Taiwan, under grant NSC 98-2221-E-109-049.

Journal of Marine Science and Technology, Vol. 24, No. 2, pp. 163-173 (2016)
DOI: 10.6119/JMST-015-0629-2

CORROSION OF REBAR UNDER CARBONATION AND SALT ENVIRONMENT

Wei-Chung Yeih, Jiang-Jhy Chang, Yu-Ping Huang, and Ran Huang

Key words: carbonation, chloride, corrosion, concrete.

ABSTRACT

In this study, the behavior of reinforced concrete under carbonation and in a salt environment was investigated. Three types of cements- Type I cement, Type II cement and high-alumina cement (HAC) - were used to study the influence of cement on reinforced concrete behavior. To simulate chloride-contaminated concrete, 1% NaCl (by cement weight) was added to some groups of specimens. Results revealed that the carbonation released chloride ions from Friedel's salt, which increased the chloride content near the carbonation front. The carbonation rate of HAC concrete was higher than that of Type I and Type II cement concrete. The corrosion rate of rebars embedded in HAC concrete was slower than that of rebars in Type I and Type II cement concrete because of the denser microstructure of HAC. However, carbonation enhanced the corrosion rate of rebars embedded in HAC concrete because of the release of chloride ions from Friedel's salt.

I. INTRODUCTION

Currently, reinforced concrete is a major construction material worldwide. Rebars compensate for the low tensile strength of concrete, and the concrete protects rebars from corrosion by providing a highly alkaline environment. However, under certain severe service conditions, the durability of reinforced concrete can be affected. Chloride attack and carbonation are critical processes that affect the durability of concrete.

Chloride ions are known to be hazardous to rebars because they destroy the passive film on the rebars once their concentration exceeds a threshold value (Ann and Song, 2007; Angst et al., 2009). Oh et al. (2003) proposed rational ranges for the threshold concentration of chloride for steel corrosion determined throiugh experiments. Chloride ions can exist in three forms in concrete: (i) free chloride; (ii) chemically bound chloride; and (iii) physically bound chloride. Generally only free chloride can cause rebar corrosion. However, chemically bound chloride and physically bound chloride can become free chloride in an appropriate environment. Increasing temperature can reduce the physically bound chloride, as mentioned in (Ann and Song, 2007). Carbonation can release the chemically bound chloride in Friedel's salt (Roper and Baweja, 1991). Arya and Xu (1995) studied the chloride binding capacity for various concrete mixtures including the ordinary Portland cement (OPC) concrete, concrete combined with ground-granulated blast-furnace slag (GGBS), concrete combined with powder fly ash (PFA), and concrete combined with silica fume (SF), and they concluded that chloride binding occurred in the order GGBS > PFA > OPC > SF. Rasheeduzzafar et al. (1993) reported that with an increase in the amount of C3A in cement, the chloride binding capability of cement also increased. Ann et al. (2010) reported that the corrosion rate in high alumina cement (HAC) mortar and concrete was lower than that in OPC concrete, despite the lower chloride binding capacity of HAC paste. Typically, the water extraction method is used to evaluate the free chloride content. By conducting experiments with various types of cement, such as OPC, high-early-strength Portland cement, moderate-heat Portland cement, calcium-aluminate cement, Type A and Type B slag cement, and Type B fly ash cement, Mohammed and Hamada observed linear relationships between free chloride and total chloride (Mohammed and Hamada, 2003).

Carbonation, also known as neutralization, reduces the pH value of a concrete pore solution, and consequently, the passive film on steel is destroyed. The destruction of the film results in the steel being corroded (Broomfield, 2000). Goñi et al. (2002) reported that the carbonation process is not influenced by the alkali of the cement and that the carbonation rate for of calcium aluminate cement is the slowest for accelerated and natural carbonation. Blenkinsop et al. (1985) studied the carbonation of HAC and claimed that the reaction rate was determined by the rapid formation of calcium carbonate and the slow precipitation of alumina hydrates. Ji et al. (2010) studied the difference between the natural carbonation process and the accelerated carbonation process and observed that the length of the semi-carbonation zone was larger for the natural carbonation process. Metalssi et al. (2014) reported that the cellulose-ether-caused delay in cement hydration delays the carbonation processes because of the lack of hydrates to react

Paper submitted 04/30/15; revised 05/30/15; accepted 06/29/15. *Author for correspondence: Jiang- Jhy Chang (e-mail: jjc@mail.ntou.edu.tw).*
Department of Harbor and River Engineering, National Taiwan Ocean University, Keelung, Taiwan, R.O.C.

with CO_2. Turcry et al. (2014) studied the influence of preconditioning through oven-drying and they concluded that the relevance of the preconditioning was questionable because it did not establish a hydric balance between the tested samples and the carbonation chamber. Moreover, the absence of carbonation close to the sample surface was revealed at an early testing stage. Dong et al. (2014) adopted electrochemical impedance spectroscopy a nondestructive testing method for studying the carbonation behavior of cementitious materials. They proposed a new electrochemical model to explain the carbonation related phenomenon. Their experimental results demonstrated that the porous structure of the cement changed and the porosity decreased during the carbonation process. Wan et al. (2014) developed a nondestructive method to characterize the 3D spatial distributions of calcium carbonate. The evolution of the calcium carbonate distributions in a cement paste specimen for various degrees of carbonation was described using this method. Based on the sharp edge of the calcium carbonate distribution, they concluded that the accelerated carbonation in this experimental condition was a diffusion-controlling process. Lo and Lee (2002) measured the carbonation depth by using a phenolphthalein indicator and infrared spectroscopy, and they reported that carbonation depths determined from the infrared spectra were 1.5 mm greater than those determined using the phenolphthalein test. Sulapha et al. (2003) studied the carbonation of concrete combined with GGBS, fly ash (FA), and SF. They reported that a decreased water-to-binder ratio and replacement level of GGBS, FA, or SF, or an increased GGBS fineness and curing age in water, led to greater carbonation resistance. However, compared with plain concrete, concrete incorporating mineral admixtures (except GGBS with higher fineness and SF) generally exhibited lower resistance to carbonation, possibly because of the dominating effect of the reduction in calcium hydroxide over pore refinement. Villain et al. (2007) compared two experimental methods for determining the carbonation depth: thermogravimetric analysis (TGA) supplemented with chemical analysis (CA) and gammadensimetry. They have concluded that TGA-CA allows $CaCO_3$ formed during C-S-H carbonation to be measured and the amount of portlandite degraded by carbonation to be calculated. Thus, total calcium carbonates profiles can be deduced even when calcareous aggregates are present in a concrete mix. Chang and Chen (2007) studied the carbonation depths measured using the TGA method, the X-ray diffraction analysis (XRDA), the Fourier transformation infrared spectroscopy (FTIR) test method and the phenolphthalein indicator method. They observed that the TGA, XRDA and FTIR results determined the depth of the carbonation front to be twice of that determined using the phenolphthalein indicator. Song and Kwon (2007) studied the capillary pore structure of a carbonated concrete, and they proposed a model to examine the capillary pore structure changes as a function of porosity under the assumption that the aggregates did not affect the carbonation process in early-aged concrete. Their proposed model was verified by examining the results of an accelerated carbonation test and a water penetration test conducted with cement mortar.

Most researches have been focused on either chloride attack or carbonation as mentioned. However, in some environments chloride attack and carbonation can occur simultaneously. Two major interactions occur between these two factors: (i) Pore structure changes resulting from carbonation (the formation of calcium carbonate) retard chloride penetration and consequent carbon dioxide penetration. (ii) Carbonation releases the chemically bound chloride in Friedel's salt leading to the formation of free chloride (Suryavanshi and Swamy, 1996; Goni and Guerrero, 2003). Al-Amoudi et al. (1991) studied the effect of salt inclusion in the OPC/PFA concrete on the concrete's alkalinity, carbonation and rebar corrosion. Their results indicated that the reduction in the alkalinity of both OPC and PFA concretes was insignificant because of chloride contamination. The corrosion of rebars was observed to be influenced more by the chloride concentrations in the concrete rather than by the presence of FA: however, the depth of carbonation was greater in FA concrete specimens compared with OPC concretes and this was ture for both chloride-free and chloride-contaminated concrete. Nepomuceno and Andrade (2006) studied the protection capacity of modified Portland cement mortar containing polymers: styrene butadiene, acrylic latex with reinforced plastic fibers and acrylic latex with SF: they used the electrochemical polarization resistance (Rp) technique to monitor the behavior of steel bars embedded in cement mortar specimens placed in CO_2 and chloride environments. They concluded that material performance depends on workability, chemical composition of squeezed pore solution porosity and resistivity which play critical roles in preventing the corrosion of steel bars. Puatatsananon and Saouma (2005) studied the nonlinear coupling effect for chloride diffusion and carbonation. Heat, relative pore humidity, chloride, and carbonation were all implemented in a 2D coupled nonlinear finite-difference code. Coupling between carbonation and chloride diffusion was investigated in the context of both homogeneous and heterogeneous concrete models. Conciatori et al. (2010) proposed the comprehensive modeling of temperature, carbonation, and water- and chloride-ions transport in cover concrete using the transport model "TransChlor". However, in their model the effect of carbonation on the chloride content (the second effect aforementioned interaction) was not considered. Montemor et al. (2002) investigated the effect of FA addition on the corrosion process occurring in reinforced concrete exposed simultaneously to carbon dioxide and chloride. They observed that under accelerated carbonation FA mortar exhibited higher corrosion rates. The chloride content of mortar exposed to accelerated carbonation increased with the amount of FA. However, under natural carbonation it decreased with the addition of FA. Wan et al. (2013) observed that carbonation had a substantial influence on the dissolved chloride content of the pore solution. After carbonation was complete the dissolved chloride content of cement mortar and hardened cement paste increased by a factor between 2 and 12. The bound chloride decreased by 27%-54%. Moreno et al. (2004) studied the cor-

Table 1. Mix design of concrete specimens.

Cement type	Water (kg/m^3)	Cement (kg/m^3)	NaCl* (kg/m^3)	Fine aggregates (kg/m^3)	Coarse aggregates (kg/m^3)
I	210	350	3.5	817	944
II	210	350	3.5	817	944
HAC	210	350	3.5	817	944

*: NaCl is used only for chloride contaminated specimens.

Table 2. Mix design of mortar specimens.

Cement type	Water (kg/m^3)	Cement (kg/m^3)	NaCl* (kg/m^3)	Fine aggregates (kg/m^3)
I	285	475	4.75	1422
II	285	475	4.75	1422
HAC	273	455	4.55	1470

*: NaCl is used only for chloride contaminated specimens

Table 3. Chemical compositions (mass percentages) for different cements.

Chemical composition	**Type I cement**	**Type II cement**	**HAC**
SiO_2	20.20	20.85	5.81
Al_2O_3	4.68	4.16	51.98
Fe_2O_3	3.10	3.95	
CaO	62.96	63.69	36.08
MgO	3.68	2.25	
SO_3	2.40	2.36	

rosion of rebars in a simulated concrete pore solution during carbonation and chloride attack. The results obtained for solutions simulating carbonated concrete pore solutions showed that under weak carbonation conditions carbon steel does not passivate: however in the presence of high levels of carbonate and bicarbonate its resistance to localized corrosion improves. Ramezanianpour et al. (2014) studied the microscopic and mechanical properties of ordinary concrete exposed to CO_2 gas, saline water, and a combination of CO_2 gas and saline water. They concluded that because of the presence of moisture in the pore solution of specimens maintained in the combined condition, low CO_2 gas and chloride ion ingression was observed.

In this study, the influence of carbonation on a chloride-contaminated concrete was investigated. The effects of various types of cement were examined and the chloride profile during carbonation was investigated. In addition, the electrochemical measurements were performed to study the corrosion status. The experimental details are provided in Section 2. In Section 3, experimental results and discussions are presented. In the final Section (Section 4), conclusions based on the experimental results are presented.

II. EXPERIMENTAL

Two types of specimens were cast: cylindrical concrete specimens with a diameter of 10 cm and a height of 20 cm and the cylindrical mortar specimens with a diameter of 5 cm and a height of 10 cm. The mix design of concrete followed ACI-211 and the designed slump was 15 cm and the air content was 2%. The mix design of the mortar had a water-to-cement ratio of 0.6, and the flowability was 100%-115%. Details of the mix designs of the concrete and mortar are tabulated in Tables 1 and 2, respectively. Using the concrete specimens and mortar specimens, we prepared control specimens (without NaCl) and chloride-contaminated specimens (containing 1% NaCl by cement weight). The chemical compositions of Type I cement, Type II cement, and HAC are listed in Table 3. The coarse aggregates used had a fineness modulus of 6.36, furthermore, the specific weight for SSD status was 2.75, the water absorption was 0.82%, and the maximum size was 19 mm. The fine aggregates had a fineness modulus of 2.63, their specific weight for SSD status was 2.59 and the water absorption was 1.39%. To investigate the corrosion status after carbonation, a 20-cm #4 rebar was embedded in the concrete specimen and a 12-cm #3 rebar was embedded in the mortar specimen.

After demolding, all specimens were cured under standard curing conditions for 28 days. They were then removed from the curing chamber and stored in air for 1 day.

Thereafter, all specimens were placed in an accelerated carbonation environment at a pressure of 15 atm and a relative humidity of 75 to 80% the concentration of CO_2 gas was 100%. After the designated carbonation period was reached, specimens were removed from the accelerated carbonation chamber and subjected to the following tests.

1. Water Absorption

Because carbonation begins from the surface, the surface properties should change more visibly compared with the properties of the entire specimen. Therefore, a water absorption test in BS 1881:122 rather than ASTM C672 was conducted. The specimen was first dried out using an oven and immersed in water for 30 minutes. After immersion, the specimen was removed from the water and the surface was wiped with a wet towel. The difference between the weight after oven-drying and that after immersion was determined. The water absorption percentage was obtained by dividing the weight difference by the weight after oven-drying and multiplying by 100.

2. Compressive Strength

The compressive strength of the cylindrical specimens was determined by following ASTM C39. It was obtained by dividing the maximum loading by the sectional area.

3. Carbonation Depth

The carbonation depth was obtained by using the phenolphthalein indicator method mentioned in RILEM CPC-18.

4. Chloride Ion Content

The sampling method presented in AASHTO T260 was followed. The water dissolved chloride content was determined using the water extraction method. The water-dissolved chloride content represented the free chloride ion content.

5. pH Value

The AASHTO T260 sampling method was used. The hydroxide ion content was determined using a method similar to that used for determining the chloride ion content. The sample was dissolved in a distilled water solution, and a titration method was used to determine the hydroxide ion content. Subsequently, the pH value was calculated.

6. Determination of Open-circuit Potential and the Corrosion Rate by Using the Linearized DC Polarization Method

The open circuit-potential for rebars embedded in the specimens was measured during the carbonation process. In addition, the corrosion rate was also monitored using the linearized DC polarization method.

7. Scanning Electron Microscope

A scanning electron microscope was used to examine the microscale changes after carbonation.

III. RESULTS AND DISCUSSIONS

1. Carbonation Depth

The carbonation depths for mortar specimens and concrete specimens are illustrated in Fig. 1(a) and 1(b), respectively. In these figures, only the influence of cement type on carbonation rate is shown. Therefore, the data obtained from uncontaminated specimens (without NaCl) were used. It was determined that the carbonation rates of HAC specimens were much higher than those of Type I and Type II cement specimens. The carbonation rates of Type II cement were slightly lower than those of Type I cement. The carbonation coefficients were 1.35, 1.27 and 13.76 mm/ $\sqrt{\text{day}}$ for Type I cement mortar, Type II cement mortar and HAC mortar, respectively. The carbonation coefficients were 4.67, 4.65 and 10.76 mm/ $\sqrt{\text{day}}$ for Type I cement concrete, Type II cement concrete and HAC concrete, respectively. The compressive strengths of HAC specimens were higher than those of Type I cement and Type II cement specimens. Generally, a higher strength concrete exhibited denser microstructure, which made the diffusion of carbon dioxide more difficult. Consequently, the carbonation coefficient was expected to be lower for a higher-strength concrete.

This phenomenon has two possible explanations. The hydration products of HAC contain fewer calcium hydroxide (CH) crystals compared with those of Type I and Type II cement.

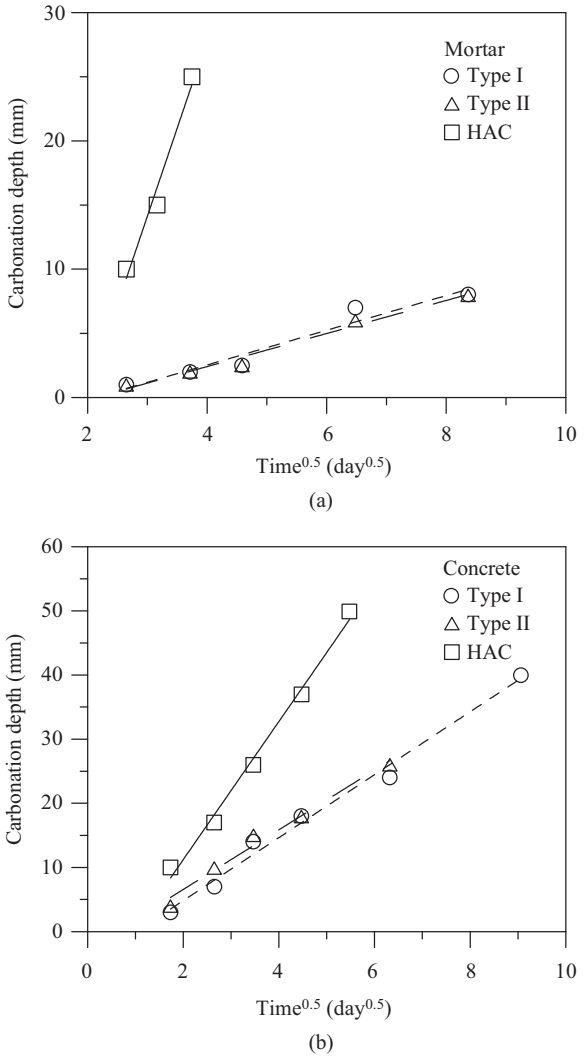

Fig. 1. The carbonation depth diagrams for (a) mortar specimens; (b) concrete specimens.

Table 4. The chloride contents and pH values for uncarbonated concrete specimens.

Cement type	I		II		HAC	
NaCl	0%	1%	0%	1%	0%	1%
pH	12.30	12.44	12.35	12.45	11.18	11.37
Cl^- (kg/m^3)	0.118	1.930	0.124	2.026	0.119	1.895

Table 5. The chloride contents and pH values for carbonated concrete specimens.

Cement type	I		II		HAC	
NaCl	1%		1%		1%	
Carbonation depth (mm)	24		26		37	
Distance from surface (mm)	pH	Cl^- (kg/m^3)	pH	Cl^- (kg/m^3)	pH	Cl^- (kg/m^3)
7	8.86	1.727	8.96	1.730	8.36	1.665
17	-	1.943	-	1.953	-	1.670
25	11.90	2.341	11.76	2.353	9.19	1.688
37	-	1.910	-	2.031	-	2.301
50	12.19	1.852	12.09	2.017	10.15	2.086

This theory can be indirectly verified by considering the results of pH value measurements presented in the next subsection. Consequently, the carbonation (or neutralization) occurred because carbon dioxide reacted with other hydrated products as mentioned in (Blenkinsop et al., 1985). Compared with the chemical reaction in the carbonation process for OPC, the reaction of carbon dioxide with CH crystals was faster.

2. Chloride Contents and pH Values

The original water dissolved chloride contents and pH values for concrete specimens before carbonation are listed in Table 4. The chloride content of HAC concrete was lower than that of Type I cement and Type II cement concrete. As show in Table 3, the order of Al_2O_3 contents of the three types of cement was in the order HAC > Type I > Type II. A higher Al_2O_3 content leads to a greater chloride binding capability. Therefore, the chloride content of HAC concrete was the lowest among the specimens prepared using the three types of cement: this finding agrees with previous studies. In addition, the order of pH values was Type II > Type I > HAC. The alkalinity of the concrete pore solution is mainly determined by the calcium ions. As shown in Table 3, the order of CaO content was Type II > Type I > HAC, which is identical to the order of pH values.

The chloride content profiles and pH values for specimens contaminated with 1% NaCl were examined after a specific period of carbonation. For Type I and Type II cement concrete, the carbonation period was 40 days. The carbonation depths were 24 mm and 26 mm for Type I and Type II cement concretes, respectively. For HAC concrete, the carbonation period was 20 days and the carbonation depth was 37 mm. The test results are tabulated in Table 5.

The chloride profiles for carbonated concretes are also presented in Fig. 2. In this figure, the red dotted lines represent the chloride content for uncarbonated concretes and the purple

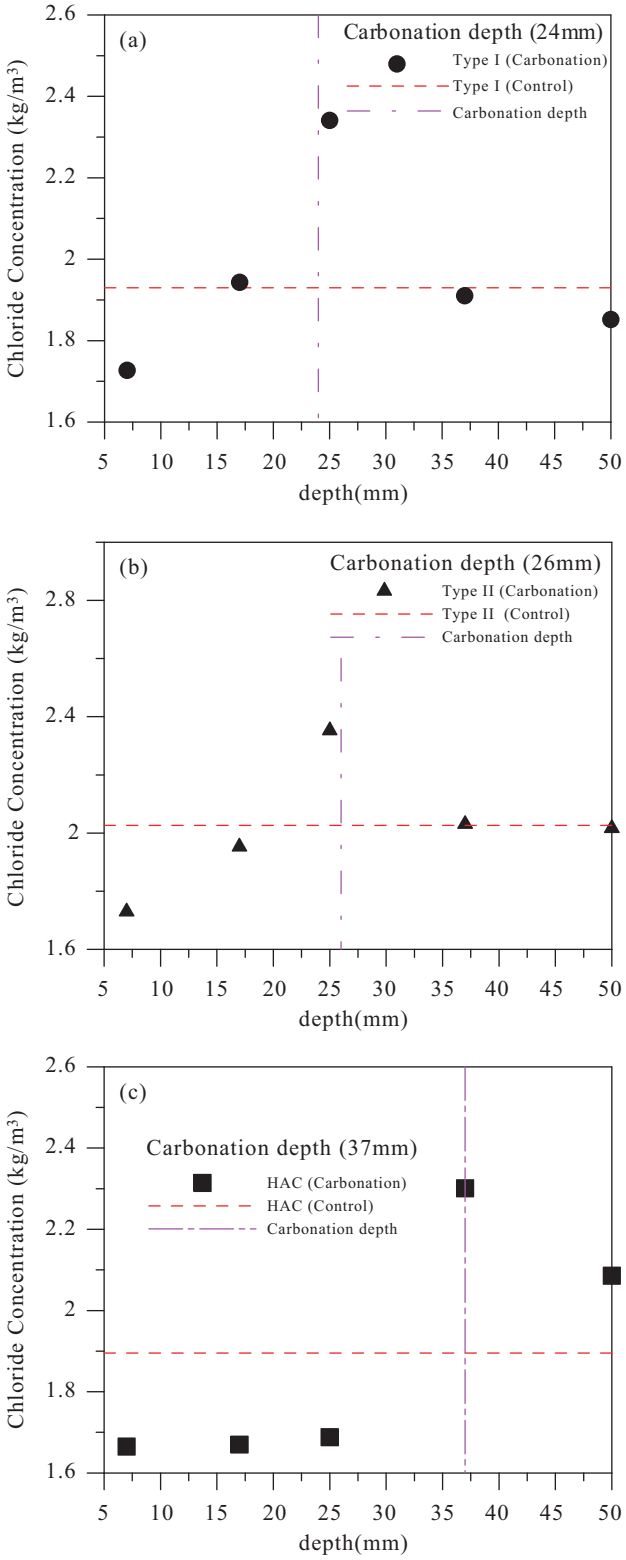

Fig. 2. The chloride profile for carbonated concretes: (a) Type I cement; (b) Type II cement; and (c) HAC.

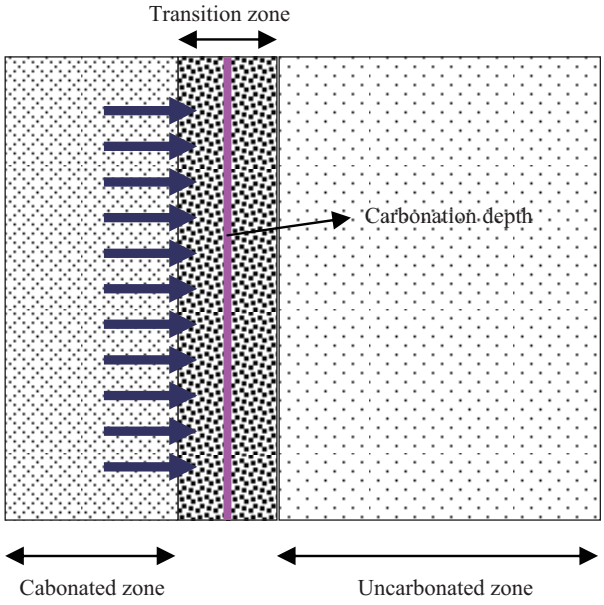

Fig. 3. The squeezing effect for cabonated zone squeezes the pore solution towards the transition zone and uncarbonated zone.

dotted lines denote the carbonation depths. Changes occurred in both chloride content and pH values near the carbonation depth. The region near the carbonation depth is recognized as a transition zone where partial carbonation occurs continuously. The reason that the pH value of this transition zone was higher than that of the carbonated zone (the zone where carbonation has been completed) but lower than the uncarbonated zone (the zone where carbonation has not begun) was the number of calcium ions in the pore solutions. In the carbonated zone, calcium hydroxide was converted to calcium carbonates. In the transition zone, partial calcium hydroixde was converted to calcium carbonates and the remaining amount of calcium hydroxide was not involved in the reaction. In the uncarbonated zone, none of the calcium hydroixde had yet undergone chemical neutralization yet. The chloride profiles suggested two mechanisms. First, for concrete that underwent carbonation the free chloride ion content increased because the release of chemically bound chloride in Friedel's salt led to the formation of free chloride: this theory has been verified in numerous studies. Second, calcium carbonate that formed condensed in the microstructure of pores and consequently, the water as well as the chloride ions were squeezed towards the transition zone and uncarbonated zone. Consequently, the chloride ion content of the transition zone was the highest that of the uncarbonated zone was the next highest and the chloride ion content of the carbonated zone was the lowest. This phenomenon was observed for all concrete specimens despite the specimens containing distinct types of cement. The aforementioned squeezing mechanism is shown in Fig. 3.

3. Compressive Strength

The compressive strengths of mortar specimens and concrete specimens during the 28-day curing period were recorded as

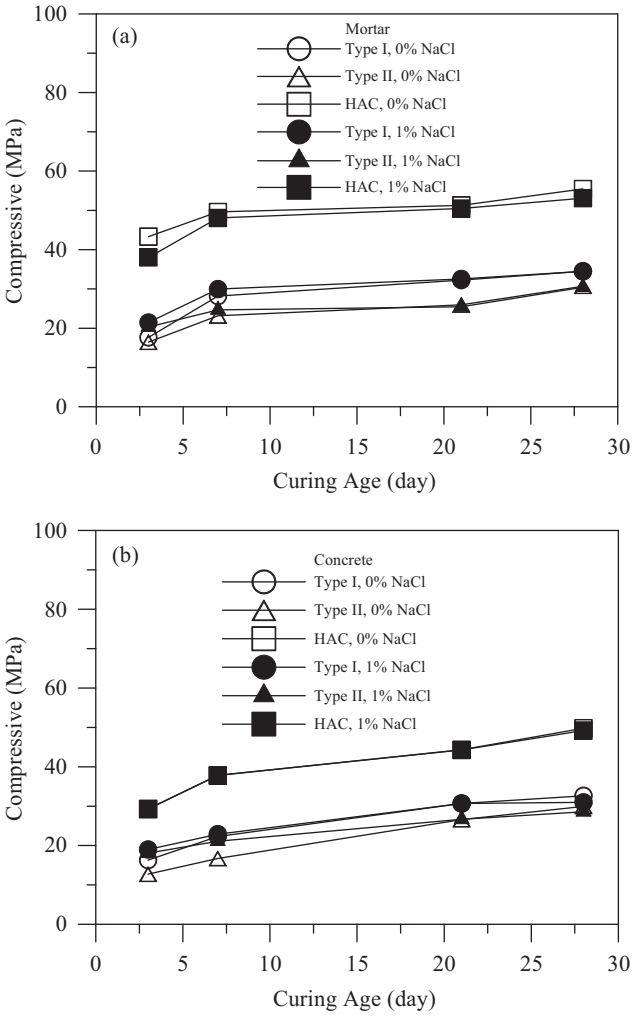

Fig. 4. Compressive strength developments for (a) mortar specimens; and (b) concrete specimens.

shown in Fig. 4(a) and 4(b), respectively. For type I and type II cement after NaCl was added to fresh concrete, the compressive strengths increased as a result of the accelerated hydration of chloride ions in a calcium-rich environment. For HAC, the addition of NaCl slightly decreased the compressive strength. As show in Table 3, the CaO content of HAC was the lowest among the three types of cement, and the CaO content was considerably low in comparison with Type I and Type II cement. Consequently, the accelerated hydration of chloride ions cannot be seen in HAC concretes. The compressive strengths of HAC concretes (or mortars) was also always higher than that of the Type I and Type II cement concretes (or mortars). Nevertheless, a higher strength did not imply a lower carbonation rate as we expected. In reality, the carbonation rate of HAC concrete was the highest.

The compressive strengths after carbonation were also recorded. For mortar specimens, the compressive strengths of Type I cement and Type II cement were recorded after 70-day carbonation whereas the compressive strength of HAC was recor-

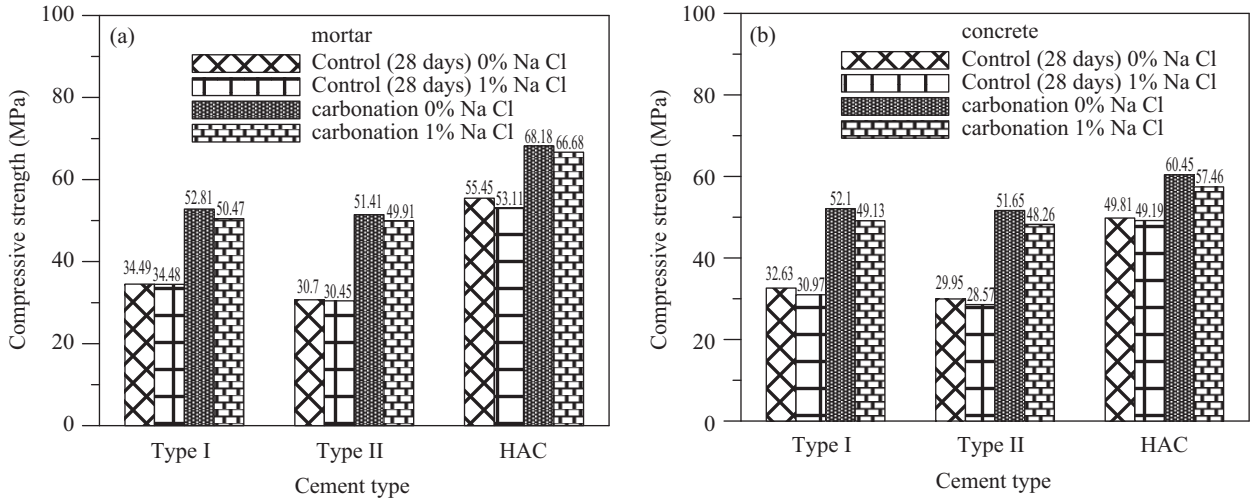

Fig. 5. The compressive strengths after carbonation: (a) mortar specimens; and (b) concrete specimens.

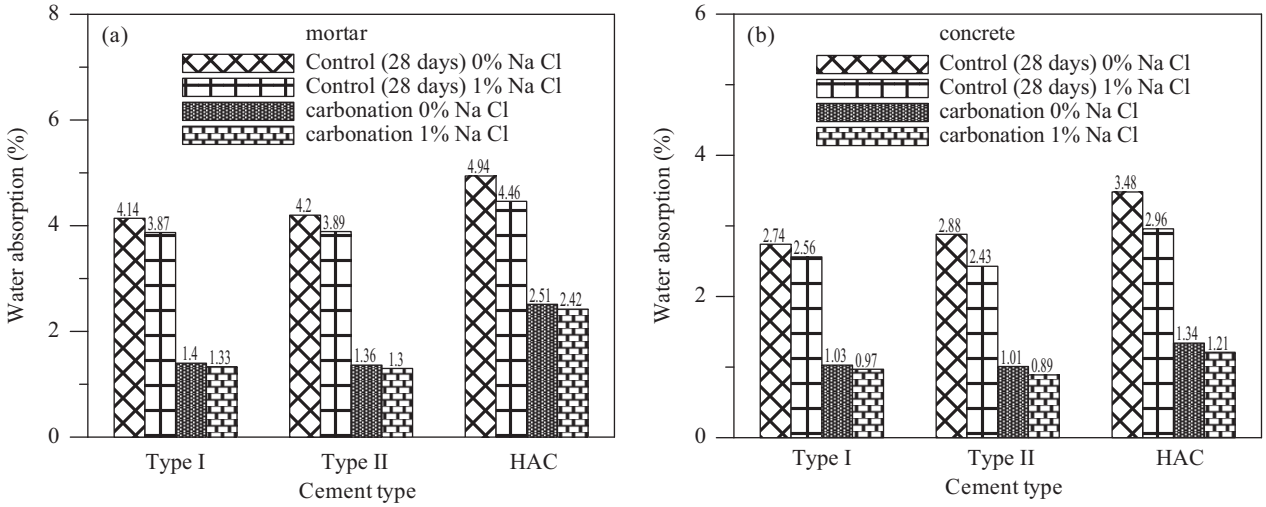

Fig. 6. Water absorptions for (a): mortar specimens; and (b) concrete specimens.

ded after 14-day carbonation. For concrete specimens, the compressive strengths of Type I cement and Type II cement were recorded after 40-day carbonation and the compressive strength of HAC was recorded after 30-day carbonation. The results are shown in Fig. 5. After carbonation, the compressive strengths increased primarily because of the carbonated products (e.g., the calcium carbonate). Moreover, the increase in strength was more apparent for Type I cement and Type II cement than for HAC. This phenomenon is based on the CaO content of various types of cement.

4. Water Absorption

The water absorption measured using the BS 1881:122 method was related to the surface porosity and microstructures of pores near the surface. Generally, if the volume of capillary pores increases, water absorption is greater. Several conclusions can be drawn from the water absorption results presented in Fig. 6: first, the addition of NaCl to fresh concrete increased the compressive strengths of Type I and Type II cement concretes. The water absorption results indicated that the addition of NaCl reduced the number of capillary pores near the surface which is in consistent with the results pertaining to compressive strengths. NaCl addition exhibited an identical effect for HAC concretes. Second, the carbonation process decreased the water absorption in all of the specimens. The decrease in water absorption stems from the blocking effect of carbonated products. In addition, water absorptions was in the order HAC > Type II > Type I. The HAC concrete exhibited the highest compressive strength. The reason why HAC show the highest water absorption was that there existed a larger amount of ettringites in hydrated products. Ettringites can absorb water and expand, and this water absorption capability was responsible for HAC concrete exhibiting the highest water absorption despite having the highest compressive strength.

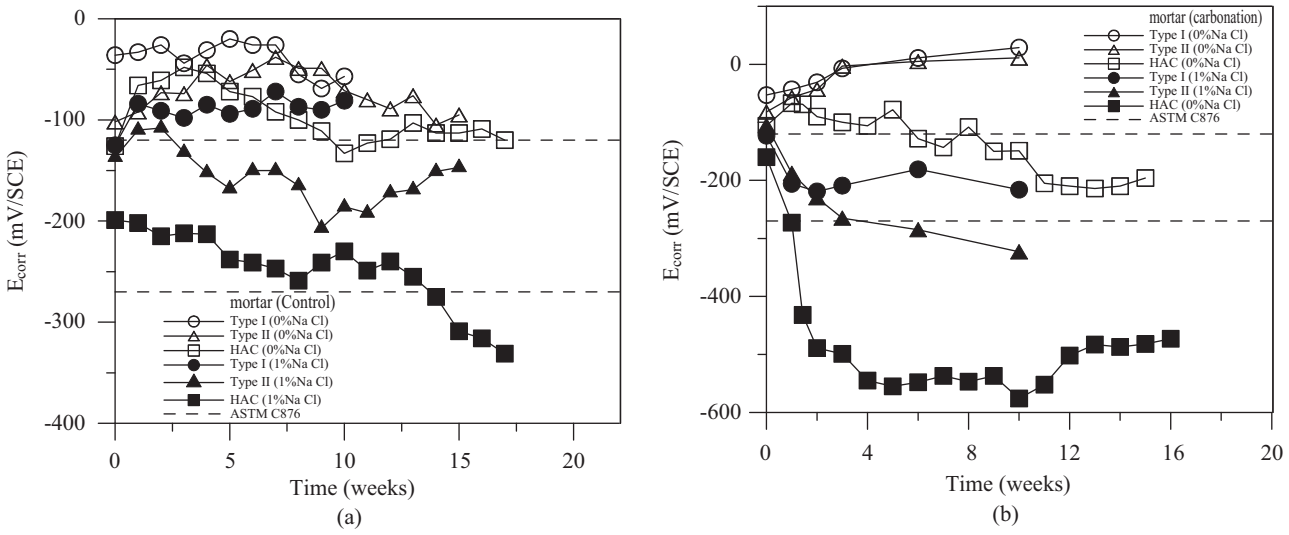

Fig. 7. The open ciruit potentials for mortar specimens: (a) uncarbonated specimens; (b) carbonated specimens.

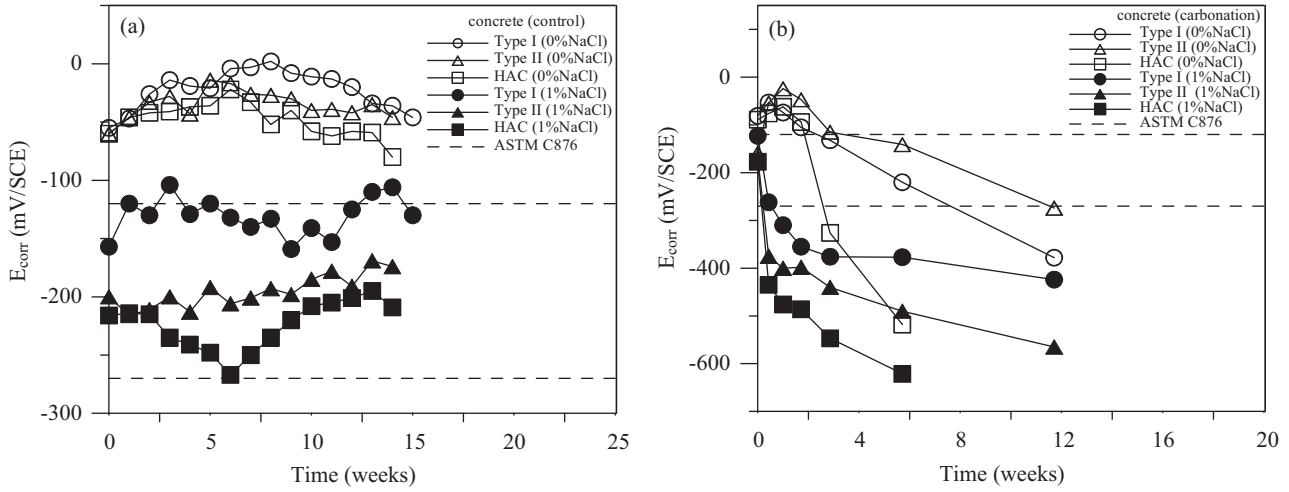

Fig. 8. The open ciruit potentials for concrete specimens: (a) uncarbonated specimens; (b) carbonated specimens.

5. Open-Circuit Potential and Corrosion Rate

The open-circuit potentials for rebars embedded in uncarbonated mortars and carbonated mortar is illustrated in Fig. 7(a) and 7(b), respectively. The open-circuit potentials for rebars embedded in uncarbonated concrete and carbonated concrete is shown in Fig. 8(a) and 8(b). In these figures, the two dotted lines denote the margin values of the open-circuit potential in ASTM C876. If the open-circuit value is higher than the noble margin value (-120 mV, SCE), the rebar corrosion probability is lower than 10%. If the open-circuit potential value is lower than the active margin value (-270 mV, SCE), the corrosion probability is higher than 90%. For an open-circuit potential is in the range of -120 mV to -270 mV, SCE, the corrosion probability of the rebar is between 10% and 90%.

The order of open-circuit potentials was Type I > Type II > HAC. The HAC specimens exhibited the most active status thermodynamically. However, HAC actually had the lowest corrosion rate among all types of cement. The open-circuit potential is affected by the steel environment. The HAC concrete contains more hydrated products of alumina which is more active than iron is. Because the Al_2O_3 content of HAC is considerably high, the open-circuit potential of rebars can be made more active by alumina. In addition, without adding chloride, the open-circuit potentials of all specimens except HAC specimens for some durations is higher than -120 mV, SCE. Adding chloride to fresh concretes made the open-circuit potential more active. The effect of carbonation can be described as the followings. For the specimens without NaCl, the carbonation made the open-circuit potential nobler because of the blocking effect of the carbonation products. For mortar specimens prepared from Type I and Type II cements, this effect of carbonation was most apparent. For chloride-contaminated specimens, carbonation generally resulted in the open-circuit

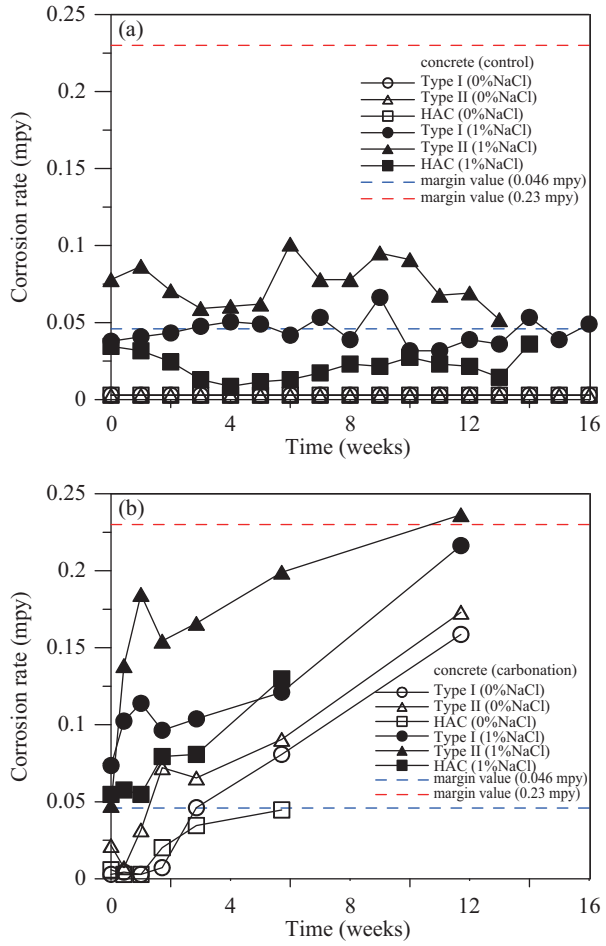

Fig. 9. The corrosion rates for concrete specimens: (a) uncarbonated specimens; (b) carbonated specimens.

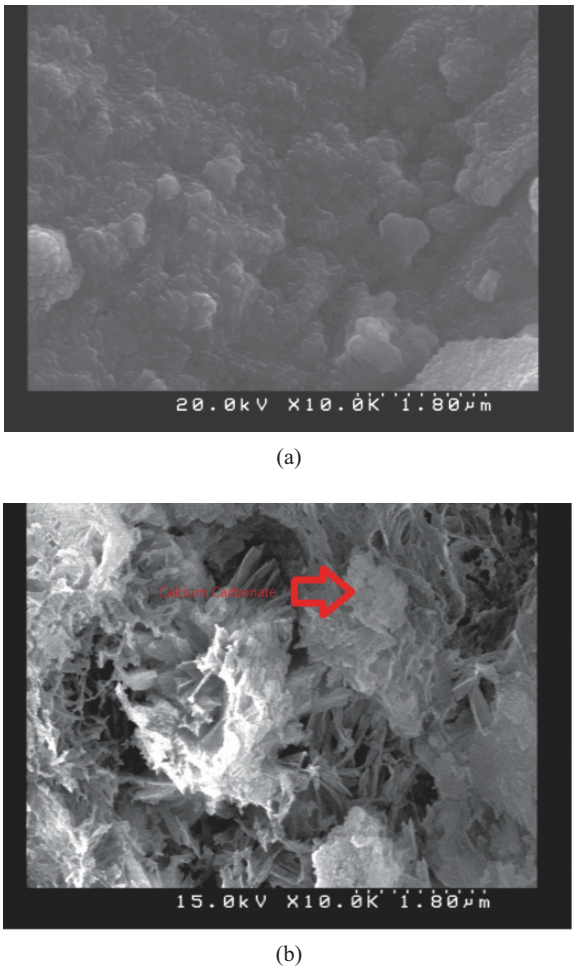

Fig. 10. The SEM photos for (a) uncarbonated concrete; and (b) carbonated concrete made by Type I cement.

potential having a tendency to have an active direction particularly when the carbonation front contracted the steel surface or was near the surface. This effect was more apparent for HAC specimens because the carbonation process increased the free chloride contents.

The corrosion rates for uncarbonated and carbonated concrete specimens are plotted in Fig. 9(a) and 9(b), respectively. In these figures, the red dotted line represents the margin value of 0.23 mpy and the blue dotted line represents the margin value of 0.046 mpy. According to Andrade and Alonso (2001), if the corrosion rate is lower than 0.046 mpy, the corrosion status is negligible. If the corrosion rate is higher than 0.046 mpy and lower than 0.23 mpy, the corrosion status is low. If the corrosion rate is higher than 0.23 mpy and lower than 0.46 mpy, the corrosion status is medium. If the corrosion rate is higher than 0.46 mpy, the corrosion status is high (Andrade and Alonso, 2001). Generally, the corrosion rates were in the following order: Type II > Type I > HAC. This order is opposite to that of compressive strengths. Higher-strength concrete has a denser microstructure that prevents the movement of reactants for oxidation as well as for reduction. Consequently, the polarization resistance of steel increases decreasing corrosion rate. Therefore, we concluded that the corrosion rates are dominated by the pore structures.

When NaCl was not added, the corrosion rates of rebars embedded in concretes prepared from all types of cement were negligible. After carbonation the corrosion rates increased with the carbonation time irrespective of whether NaCl was added. Although the carbonation rate of HAC concrete was the highest its corrosion rate was the lowest. When HAC concrete was carbonated, the chloride was squeezed toward the transition zone and the uncarbonated zone. In addition, the pH value of the carbonated zone decreased. These two factors increased the corrosion rates of rebars. However, even when the carbonation depth reached the rebar the corrosion status of the rebar continued to depend on the polarization resistance (which was determined by Tafel's slopes for the anode and cathode). The pore microstructure in HAC concrete dominated the resistance.

6. Scanning Electron Microscopy

Scanning electron microscope images for uncarbonated and carbonated concrete prepared from Type I cement are shown in Fig. 10(a) and 10(b), respectively.

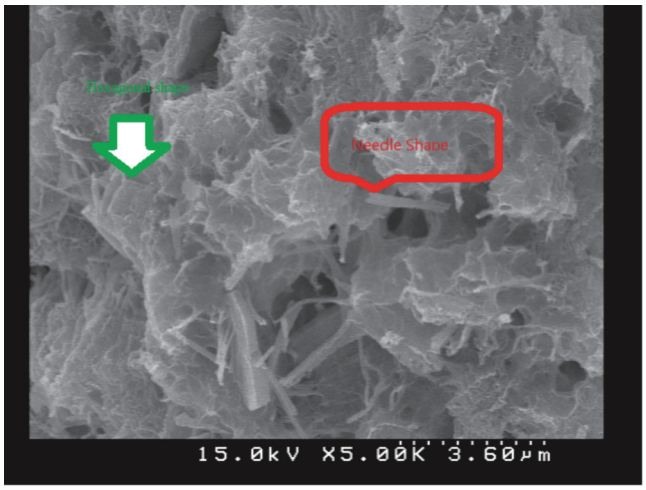

(a)

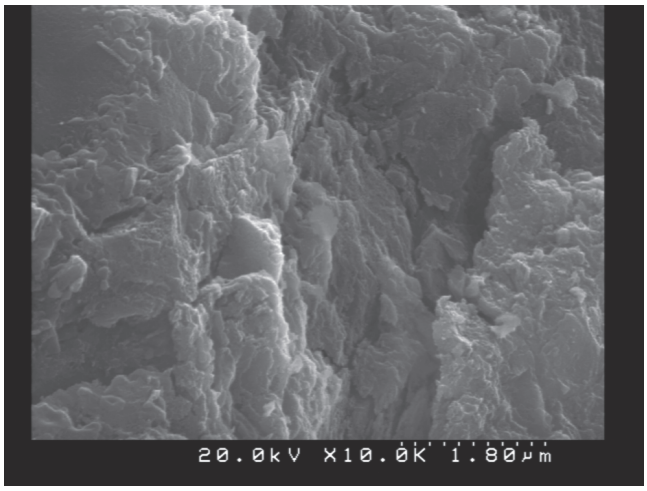

(b)

Fig. 11. SEM photos for (a) uncarbonated HAC concrete; and (b) carbonated HAC concrete.

Cubic calcium carbonate crystals were observed in the carbonated concrete. The formation of calcium carbonate explains the blocking effect of carbonation. Images of uncarbonated and carbonated HAC are shown in Fig. 11(a) and 11(b), respectively. Hexagonal thin sheets (calcium monosulfoaluminate) and needle shapes (ettringite) can be clearly observed in the uncarbonated concrete. Ettringite can absorb water, and consequently its volume expands. This micro-scale image supports the explanation of the higher water absorption of HAC concretes.

IV. CONCLUSIONS

In this study, the behavior of reinforced concrete under carbonation and in a salt environment was investigated. Type I cement, Type II cement and HAC were used to study the influence of Al_2O_3. The results revealed that HAC concrete exhibited the highest compressive strength, the highest water absorption and the highest carbonation rate. However, the corrosion rate of HAC concrete was the lowest. During carbonation, the highest chloride content was observed near the carbonation front. A squeezing mechanism is proposed to explain this phenomenon. The corrosion rate was dominantly controlled by the pore structure and therefore, the electrochemical polarization resistance of the concrete specimens differed with the type of cement for their preparation.

ACKNOWLEDGMENTS

This work was supported by National Science Council, Taiwan, under grant NSC 98-2221-E-109-049.

REFERENCES

Andrade, C. and C. Alonso (2001). On-site measurement of corrosion rate of reinforcements. Construction and Building Materials 15, 141-145.

Angst, U., B. Elsener, C. K. Larsen and Ø. Vennesland (2009). Critical chloride content in reinforced concrete — A review. Cement and Concrete Research 39(12), 1122-1138.

Ann, K. Y. and H. W. Song (2007). Chloride threshold level for corrosion of steel in concrete. Corrosion Science 49(11), 4113-4133.

Ann, K. Y., T. S. Kim, J. H. Kim and S. H. Kim (2010). The resistance of high alumina cement against corrosion of steel in concrete. Construction and Building Materials 24(8), 1502-1510.

Al-Amoudi, O. S. B., Rasheeduzzafar and M. Maslehuddin (1991). Carbonation and corrosion of rebars in salt contaminated OPC/PFA concretes. Cement and Concrete Research 21(1), 38-50.

Arya, C. and Y. Xu (1995). Effect of cement type on chloride binding and corrosion of steel in concrete. Cement and Concrete Research 25(4), 893-902.

Blenkinsop, R. D., B. R. Currell, H. G. Midgley and J. R. Parsonage (1985). The carbonation of high alumina cement, part I. Cement and Concrete Research 15(2), 276-284.

Broomfield, J. P. (2000). Carbonation and its effects in reinforced concrete. Materials Performance 39(1).

Chang, C. F. and J. W. Chen (2007). The experimental investigation of concrete carbonation depth. Cement and Concrete Research 37, 1182-1192.

Conciatori, D., F. Laferrière and E. Brühwiler (2010). Comprehensive modeling of chloride ion and water ingress into concrete considering thermal and carbonation state for real climate. Cement and Concrete Research 40(1), 109-118.

Dong, B. Q., Q. W. Qiu, J. Q. Xiang, C. J. Huang, F. Xing, N. X. Han and Y. Y. Lu (2014). Electrochemical impedance measurement and modeling analysis of the carbonation behavior for cementititous materials. Construction and Building Materials 54, 558-565.

Goñi, S., M. T. Gaztañaga and A. Guerrero (2002). Role of cement type on carbonation attack. Journal of Materials Research 17(7), 1834-1842.

Goñi, S. and A. Guerrero (2003). Accelerated carbonation of Friedel's salt in calcium aluminate cement paste. Cement and Concrete Research 33(1), 21-26.

Ji, Y., Y. Yuan, J. Shen, Y. Ma and S. Lai (2010). Comparison of concrete carbonation process under natural condition and high CO_2 concentration environments. Journal of Wuhan University of Technology-Material Scence Ed. 25(3), 515-522.

Lo, Y. and H. M. Lee (2002). Curing effects on carbonation of concrete using a phenolphthalein indicator and Fourier-transform infrared spectroscopy. Building and Environment 37(5), 507-514.

Metalssi, O. O., A. Aït-Mokhtar and B. Ruot (2014). Influence of cellulose ether on hydration and carbonation kinetics of mortars. Cement and Concrete Composites 49, 20-25.

Mohammed, T. U. and H. Hamada (2003). Relationship between free chloride and total chloride contents in concrete. Cement and Concrete Research 33(9), 1487-1490.

Montemor, M. F., M. P. Cunha, M. G. Ferreira and A. M. Simões (2002). Corrosion behaviour of rebars in fly ash mortar exposed to carbon dioxide and chlorides. Cement and Concrete Composites 24(1), 45-53.

Moreno, M., W. Morris, M. G. Alvarez and G. S. Duffó (2004). Corrosion of reinforcing steel in simulated concrete pore solutions: Effect of carbonation and chloride content. Corrosion Science 46(11), 2681-2699.

Nepomuceno, A. A. and C. Andrade (2006). Steel protection capacity of polymeric based cement mortars against chloride and carbonation attacks studied using electrochemical polarization resistance. Cement and Concrete Composites 28(8), 716-721.

Oh, B. H., S. Y. Jang and Y. S. Shin (2003). Experimental investigation of the threshold chloride concentration for corrosion initiation in reinforced concrete structures. Magazine of Concrete Research 55(2), 117-124.

Puatatsananon, W. and V. Saouma (2005). Nonlinear Coupling of Carbonation and Chloride Diffusion in Concrete. Journal of Material Civil Engineering 17(3), 264-275.

Ramezanianpour, A. A., S. A. Ghahari and M. Esmaeili (2014). Effect of combined carbonation and chloride ion ingress by an accelerated test method on microscopic and mechanical properties of concrete. Construction and Building Materials 58(15), 138-146.

Rasheeduzzafar, S., S. E. Hussain and S. S. Al-Saadoun (1993). Effect of Tricalcium Aluminate Content of Cement on Chloride Binding Corrosion of Reinforcing Steel in Concrete. ACI Materials Journal 89(1), 3-12.

Roper, H. and D. Baweja (1991). Carbonation-Chloride Interactions and Their Influence Corrosion Rates of Steel in Concrete. ACI Special Publication 126, 295-316.

Song, H. W. and S. J. Kwon (2007). Permeability characteristics of carbonated concrete considering capillary pore structure. Cement and Concrete Research 37(6), 909-915.

Sulapha, P., S. Wong, T. Wee and S. Swaddiwudhipong (2003). Carbonation of Concrete Containing Mineral Admixtures. Journal of Material Civil Engineering 15(2), 134-143.

Suryavanshi, A. K. and R. N. Swamy (1996). Stability of Friedel's salt in carbonated concrete structural elements. Cement and Concrete Research, 26(5) 729-741.

Turcry, P., L. Oksri-Nelfia, A. Younsi and A. Aït-Mokhtar (2014). Analysis of an accelerated carbonation test with severe preconditioning. Cement and Concrete Research 57, 70-78.

Villain, G., M. Thiery and G. Platret (2007). Measurement methods of carbonation profiles in concrete: Thermogravimetry, chemical analysis and gammadensimetry. Cement and Concrete Research 37, 1182-1192.

Wan, K., Q. Xu, Y. Wang and G. Pan (2014). 3D spatial distribution of the calcium carbonate caused by carbonation of cement paste. Cement and Concrete Composites 45, 255-263.

Wan, X. M., F. H. Wittmann, T. J. Zhao and H. Fan (2013). Chloride content and pH value in the pore solution of concrete under carbonation. Journal of Zhejiang University SCIENCE A 14(1), 71-78.